Progress In Electromagnetics Research Letters, Vol. 43, 73–81, 2013

3D SUPER-RESOLUTION FLUORESCENCE MICROSCOPY USING CYLINDRICAL VECTOR BEAMS

Taikei Suyama[1] and Yaoju Zhang[2, *]

[1]Department of Electrical and Computer Engineering, Akashi National College of Technology, Akashi 674-8501, Japan

[2]College of Physics and Electronic Information, Wenzhou University, Wenzhou 325035, China

Abstract—We propose a method to obtain nano-scale 3D super-resolution in STED fluorescence microscopy. A double-ring-shaped cylindrical vector vortex beam, with an appropriate vortex angle and a proper truncation parameter of the beam, is used to generate a 3D dark spot as the erase spot. A single-ring-shaped radially polarized beam is used as a pump beam, which can generate a sharper 3D bright spot. The volume of the generated 3D dark spot is small and the uniformity of the light wall surrounding the spot is quite high. Consequently, the 3D super-resolution ability of a STED microscope is improved and nano-scale three-dimensional resolutions are obtained.

1. INTRODUCTION

Three-dimensional (3D) dark spots surrounded by light (bottle beams) are applied in many areas in optics, such as dark-spot optical traps for atoms [1, 2] or as erase beams for super-resolution fluorescence microscopy [3–7]. Several methods have been used to produce 3D bottle beams that have an intensity null surrounded by light in all directions. Some of these approaches require optical access from several sides or the use of custom optical polarization plates, holograms, or spatial light modulators. A simple method to create a 3D bottle beam is to use a double-ring-shaped radially polarized beam (R-TEM_{11}*) [8]. The R-TEM_{11}* beam can also be applied to improve the depth of focus in near-field optical storage [9, 10]. However, a serious drawback of the R-TEM_{11}* method is that the maximum light intensity surrounding the dark focal spot is much lower in the diagonal

Received 2 August 2013, Accepted 26 September 2013, Scheduled 30 September 2013

* Corresponding author: Yaoju Zhang (zhangyaoju@sohu.com).

direction in the light meridian plane than along the optical axis (see Figure 3(a) in Ref. [8]) and the uniformity in the intensity of the light "wall" surrounding the 3D dark spot is about 0.35. Similar phenomena also exist in interference generation of an optical bottle beam trap by interfering two fundamental Gaussian beams with different waists [2], and in the circular two-zone π-phase plate method to create a 3D bottle beam wherein the maximum light intensity surrounding the dark focal spot is much lower in the transverse directions than along the optical axis [11, 12]. If such beams are used as the erase beam in super-resolution fluorescence microscopy, the overall erase beam power cannot be increased to induce efficient fluorescence depletion in the diagonal direction without causing photo-damage along the axial direction, and consequently the resolution in the diagonal direction is limited to a relatively small value. In addition, in dark traps for atoms or biological particles, the depth of the trap is determined by the minimal intensity of the light wall, hence high non-uniformity reduces the trap depth for a given laser power.

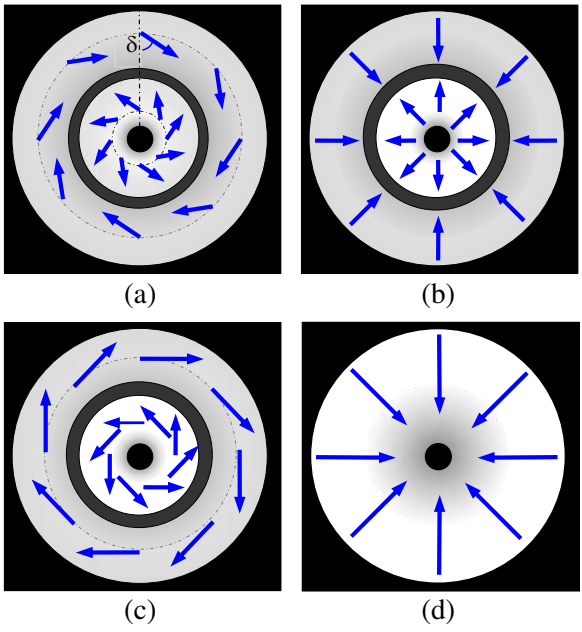

Figure 1. The instantaneous polarization states. (a) A general double-ring-shaped cylindrical vector vortex beams with vortex angle δ, (b) a double-ring-shaped radially polarized beam, (c) a double-ring-shaped azimuthally polarized beam, and (d) a single-ring-shaped radially polarized beam.

In this study, we used a highly focused double-ring-shaped cylindrical vector vortex beam with an appropriate vortex angle and a proper truncation parameter to generate a 3D dark spot. The volume of the generated 3D dark spot is very small and the light wall surrounding it has high uniformity. A small 3D bright spot is generated using a highly focused single-ring-shaped radially polarized beam. The generated 3D dark and bright spots are used as the erase and pump beams respectively in Stimulated Emission Depletion (STED) fluorescence microscopy, yielding high 3D super-resolution.

2. ERASE BEAM AND PUMP BEAM

Figure 1(a) shows the instantaneous polarization state of a general double-ring-shaped cylindrical vector vortex beam with vortex angle δ, which can be generated directly inside a laser cavity [13] or outside the laser cavity [14]. We will show that after focusing by a high numerical aperture (NA) objective, this vortex beam can generate a small three-dimensional dark spot uniformly surrounded by light, which can be used as the erase spot of a two color far-field three-dimensional super-resolution microscope [3]. This vortex beam can be considered to be the coherent superposition of two radially (Figure 1(b)) and azimuthally (Figure 1(c)) polarized beams. When a double-ring-shaped cylindrical vector vortex beam is incident on a high NA lens, the electric fields in the focal region can be obtained according to vector diffraction theory [15] as:

$$E_r^e(r,z) = \eta_e \cos\delta \int_0^\alpha \sqrt{\cos\theta} A_1(\theta) \sin 2\theta J_1(k_e r \sin\theta) \exp(ik_e z \cos\theta) d\theta, \quad (1)$$

$$E_\varphi^e(r,z) = 2\eta_e \sin\delta \int_0^\alpha \sqrt{\cos\theta} A_1(\theta) \sin\theta J_1(k_e r \sin\theta) \exp(ik_e z \cos\theta) d\theta, \quad (2)$$

$$E_z^e(r,z) = 2i\eta_e \cos\delta \int_0^\alpha \sqrt{\cos\theta} A_1(\theta) \sin^2\theta J_0(k_e r \sin\theta) \exp(ik_e z \cos\theta) d\theta. \quad (3)$$

Thus, the intensity of the erase beam can be written as

$$I_e = |E_r^e(r,z)|^2 + |E_\varphi^e(r,z)|^2 + |E_z^e(r,z)|^2. \quad (4)$$

A single-ring-shaped conventional radially polarized beam, as shown in Figure 1(d), is used as the pump light beam for exciting fluorescence. The electric fields of the pump beam in the focal region can be expressed as:

$$E_r^p(r,z) = \eta_p \int_0^\alpha \sqrt{\cos\theta} A_0(\theta) \sin 2\theta J_1(k_{p1} r \sin\theta) \exp(ik_p z \cos\theta) d\theta, \quad (5)$$

$$E_z^p(r,z) = 2i\eta_p \int_0^\alpha \sqrt{\cos\theta} A_0(\theta) \sin^2\theta J_0(k_p r \sin\theta) \exp(ik_p z \cos\theta) d\theta. \quad (6)$$

The intensity of fluorescence excited by the pump beam can be written as:

$$I_p = |E_r^p(r,z)|^2 + |E_z^p(r,z)|^2. \quad (7)$$

In Eqs. (1)–(3), (5) and (6), $k_e = 2\pi n/\lambda_e$ and $k_p = 2\pi n/\lambda_p$ are the wavenumbers of the erase and pump beams, respectively, in the immersion liquid with refractive index n. We have assumed that the wavelength of the fluorescence is the same as that of the pump beam. J_n is the nth-order Bessel function of the first kind, (r, φ, z) are the cylindrical coordinates centered at the geometric focus, and the optical axis is along the z axis. η_e and η_p are constants related to the power of the erase and pump lasers, respectively. $A_p(\theta)$ represents the amplitude distribution at the exit pupil of the objective, which can be expressed as Eq. (8):

$$A_p(\theta) = \frac{\beta \sin\theta}{\sin\alpha} \exp\left[-\left(\frac{\beta \sin\theta}{\sin\alpha}\right)^2\right] L_p^1\left[2\left(\frac{\beta \sin\theta}{\sin\alpha}\right)^2\right], \; p = 0 \text{ and } 1, \quad (8)$$

where L_p^1 is the generalized Laguerre polynomial with $p+1$ rings and $\beta = R/w$ is called the truncation parameter where w is the waist of the Gauss beam and R is the radius of the aperture inserted at the front of the objective. For the double-ring-shaped radially polarized beam, β should be larger than 1 because the outer ring of the beam will be completely blocked by the pupil if $\beta < 1$. From the above formula, it is immediately found that the intensity distribution in the focal region is rotationally symmetric with respect to the optical axis, whether for the erase beam focusing or for the pump beam focusing.

Figure 2 shows the intensity distribution of the highly focused erase beam in the x-z plane. In the calculations, we assumed that the fluorescent microspheres are immersed in oil with refractive index $n = 1.515$. The wavelength of the erase laser is 599 nm, which is sufficiently far from the fluorescence band of the microspheres to mainly contribute to the up-conversion process and not to the stimulated emission [16]. The imaging system has a high numerical aperture of NA$(= n\sin\alpha) = 1.48$ to achieve high resolution. The truncation parameter β of the erase beam equals 1.3 to form a 3D dark spot. The vortex angle of the erase beam was chosen to be $\delta = 45^\circ$ so that the light wall surrounding the 3D dark spot has high uniformity. From Figure 2, it can be seen that the double-ring-shaped cylindrical vector vortex with $\beta = 1.3$ and $\delta = 45^\circ$ can generate a perfect 3D dark spot, and the lowest intensity of the light wall is in the diagonal direction. The volume of this 3D dark spot

is very small and the light wall surrounding it is quite uniform. If the uniformity of the light wall is defined as the ratio of the lowest intensity in the light wall to the highest intensity in the light wall, we find that the uniformity of the light wall in Figure 2 is 0.66 with a double-ring-shaped vortex beam, which is much larger than the value of 0.35 with the R-TEM$_{11}$* beam method [8] or a two-zone phase element method [11, 12]. If the uniformity of the light wall is too small, the overall erase beam power cannot be increased to induce efficient fluorescence depletion in the direction of the lowest intensity in the light wall without causing photo-damage in the direction of the highest intensity in the light wall, limiting the super-resolution in the transverse direction to a relatively small factor. Therefore, the 3D dark spot with a fairly uniform light wall in Figure 2 can improve the resolution of a fluorescence microscope.

Figure 3 shows the intensity distribution of fluorescence excited by a highly focused pump beam in the x-z plane without the erase beam. We assume that the microspheres exhibit relatively strong emission at a wavelength close to 532 nm. Therefore, the wavelength of the pump laser is chosen to be 532 nm. The waist and truncation parameter are the same as those of the erase beam. It is clear that a small 3D bright spot is generated with a single-ring-shaped R-TEM$_{11}$* beam.

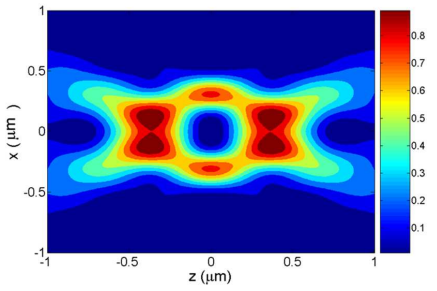

Figure 2. Normalized intensity distribution in the x-z plane for a highly focused double-ring-shaped vortex beam with vortex angle of 45°.

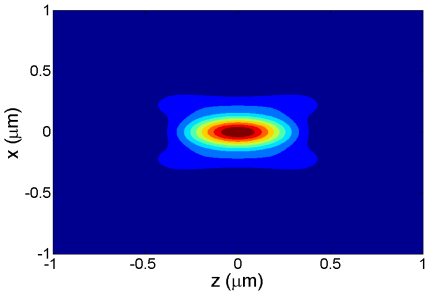

Figure 3. Normalized intensity distribution of fluorescence excited by a highly focused single-ring-shaped radially polarized beam in the x-z plane without an erase beam.

3. 3D SUPER-RESOLUTION IN STED MICROSCOPY

Figure 4 shows the schematic plot of a 3D STED fluorescence microscopy. The erase beam is a double-ring-shaped cylindrical vector

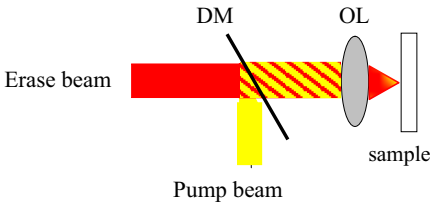

Figure 4. Schematic plot of the set-up for a 3D STED fluorescence microscopy. DM — dichroic mirror. OL — objective lens.

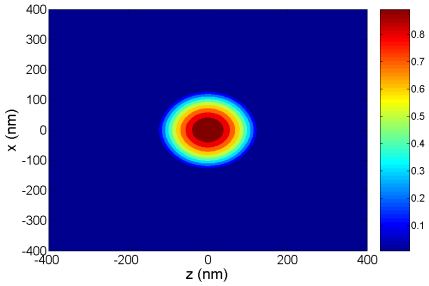

Figure 5. Normalized fluorescence intensity distribution in the x-z plane with an erase beam of $\gamma = 4$ in the designed STED fluorescence microscopy system.

vortex beam which can generate a 3D dark spot in the focal region. The pump beam to excite fluorescence is a single-ring-shaped R-TEM$_{11}$* beam, which can generate a 3D bright spot in the focal region. The erase and pump beams are incoherently overlaid by a dichroic mirror (DM). The overlaid beam is focused by the objective lens (OL). The sample labeled with fluorescent dyes is placed close to the focus.

When the erase beam exists, the fluorescence intensity distribution in fluorescence depletion microscopy can be calculated as:

$$I_f(r,z) = I_p(r,z) - I_e(r,z), \text{ when } I_p \geq I_e. \tag{9}$$

It is known that in super-resolution STED fluorescence microscopy, the FWHM of the resulting spot depends on the saturation factor γ [17, 18],

$$\gamma = I_{\text{STED}}/I_S, \tag{10}$$

where I_{STED} is the light-wall intensity of the dark spot and I_S the effective saturation intensity, which can be defined as the intensity at which the probability of fluorescence emission is reduced by half. It should be pointed out that if the intensity of the light wall surrounding a 3D dark spot is not uniform, I_{STED} is equal to the lowest intensity in the light wall rather than the highest intensity. Figure 5 shows the normalized fluorescence intensity distribution in the x-z plane when $\gamma = 4$. From this figure, the transverse and axial FWHMs of the 3D fluorescent spot are found to be 164 nm (0.31λ) and 158 nm (0.29λ), which are much smaller than the FWHMs of 219 nm (0.61λ/NA) and 485 nm (2λ/NA^2) respectively in the conventional microscopy system. It is clear that 3D super-resolution is achieved using the designed fluorescent depletion microscopy system.

Further, this microscopy system can theoretically generate an arbitrarily small 3D spot, if only the saturation factor γ is sufficiently large. Figure 6 shows the FWHM of the fluorescence spot size as a function of γ. As γ increases, the 3D spot size rapidly decreases. For example, when $\gamma = 150$, the transverse and axial FWHMs of the 3D spot are 59.9 nm (about $\lambda/9$) and 12.5 nm (about $\lambda/42$) respectively. In addition, it is seen that when $\gamma < 3.335$, the transverse FWHM is smaller than the axial FWHM. When $\gamma > 3.335$, however, the axial FWHM is smaller than the transverse FWHM, which implies that in general, the axial super-resolving ability of the system is stronger than the transverse super-resolving ability for the designed STED fluorescence microscopy system.

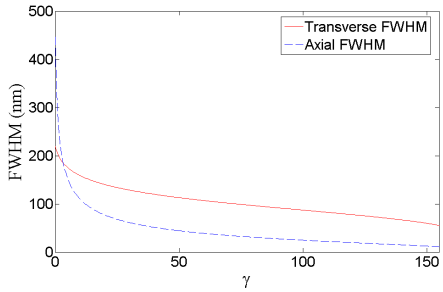

Figure 6. Dependence of the spot size FWHM in the super-resolution fluorescent microscopy system on the saturation factor γ. The solid and dashed curves are the spot sizes in the transverse and axial directions, respectively.

4. CONCLUSIONS

We propose a method to obtain 3D super-resolution in STED fluorescence microscopy. In our method, a double-ring-shaped cylindrical vector vortex beam with an appropriate vortex angle and truncation parameter of the beam is used to generate a 3D dark spot as the erase spot. The volume of the 3D dark spot generated is small, and the uniformity of the light wall surrounding it is quite high, reaching 0.66, both of which are very useful for improving the 3D resolution of a STED microscope. A single-ring-shaped radially polarized beam is used as a pump beam, which can generate a sharper 3D bright spot. Theoretically, arbitrary high 3D resolution, for example, spot size is $\lambda/9$ in the transverse direction and $\lambda/42$ along the optical axis when the saturation factor is equal to 150, can be achieved

using the designed fluorescence microscopy system. According to the requirements, the resolution can be arbitrarily changed by simply adjusting the saturation factor.

ACKNOWLEDGMENT

This work was supported by the National Natural Science Foundation of China (Grants Nos. 61078023 and 61377021) and the Public Welfare Project of Zhejiang Province science and technology office (Grant No. 2010C31051).

REFERENCES

1. Kaplan, A., N. Friedman, and N. Davidson, "Optimized single-beam dark optical trap," *J. Opt. Soc. Am. B*, Vol. 19, 1233–1238, 2002.
2. Isenhower, L., W. Williams, A. Dally, and M. Saffman, "Atom trapping in an interferometrically generated bottle beam trap," *Opt. Lett.*, Vol. 34, 1159–1161, 2009.
3. Watanabe, T., Y. Iketaki, T. Omatsu, K. Yamamoto, M. Sakai, and M. Fujii, "Two-point-separation in super-resolution fluorescence microscope based on up-conversion fluorescence depletion technique," *Opt. Express*, Vol. 11, 3271–3276, 2003.
4. Hell, S. W. "Far-field optical nanoscopy," *Science*, Vol. 316, 1153–1158, 2007.
5. Lotito, V., U. Sennhauser, C. V. Hafner, and G.-L. Bona, "Interaction of an asymmetric scanning near field optical microscopy probe with fluorescent molecules," *Progress In Electromagnetics Research*, Vol. 121, 281–299, 2011.
6. Liao, C.-C. and Y.-L. Lo, "Phenomenological model combining dipole-interaction signal and background effects for analyzing modulated detection in apertureless scanning near-field optical microscopy," *Progress In Electromagnetics Research*, Vol. 112, 415–440, 2011.
7. Di Donato, A., A. Morini, and M. Farina, "Optical fiber extrinsic micro-cavity scanning microscopy," *Progress In Electromagnetics Research*, Vol. 133, 347–366, 2013.
8. Zhang, Y., B. Ding, and T. Suyama, "Trapping two types of particles using a double-ring-shaped radially polarized beam," *Phys. Rev. A*, Vol. 81, 023831, 2010.
9. Zhang, Y. and J. Bai, "Improving the recording ability of a near-

field optical storage system by higher-order radially polarized beams," *Opt. Express*, Vol. 17, 3698–3706, 2009.

10. Zhang, Y., Y. Okuno, and X. Xu, "Theoretical study of optical recording with a solid immersion lens illuminated by focused double-ring-shaped radially polarized beam," *Opt. Commun.*, Vol. 282, 4481–4485, 2009.
11. Ozeri, R., L. Khaykovich, and N. Davidson, "Long spin relaxation times in a single-beam blue-detuned optical trap," *Phys. Rev. A*, Vol. 59, R1750–R1753, 1999.
12. Bokor, N. and N. Davidson, "Tight parabolic dark spot with high numerical aperture focusing with a circular π phase plate," *Opt. Commun.*, Vol. 270, 145–150, 2007.
13. Moser, T., H. Glur, V. Romano, F. Pigeon, O. Parriaux, M. A. Ahmed, and T. Graf, "Polarization-selective grating mirrors used in the generation of radial polarization," *Appl. Phys. B*, Vol. 80, 707–713, 2005.
14. Yonezawa, K., Y. Kozawa, and S. Sato, "Generation of a radially polarized laser beam by use of the birefringence of a c-cut Nd:YVO_4 crystal," *Opt. Lett.*, Vol. 31, 2151–2153, 2006.
15. Youngworth, K. S. and T. G. Brown, "Focusing of high numerical aperture cylindrical-vector beams," *Opt. Express*, Vol. 7, 77–87, 2000.
16. Sahar, E. and D. Treves, "Excitation singlet-state absorption in dyes and their effect on dyes lasers," *IEEE J. Quntum Electronics*, Vol. 13, 962–967, 1977.
17. Westphal, V. and S. W. Hell, "Nanoscale resolution in the focal plane of an optical microscope," *Phy. Rev. Lett.*, Vol. 94, 143903, 2005.
18. Harke, B., J. Keller, C. K. Ullal, V. Westphal, A. Schönle, and S. W. Hell, "Resolution scaling in STED microscopy," *Opt. Express*, Vol. 16, 4154–4162, 2008.